Endogenous Tryptophan-Derived Ah Receptor Ligands are Dissociated from CYP1A1/1B1-Dependent Negative-Feedback

International Journal of Tryptophan Research
Volume 16: 1–11

DOI: 10.1177/11786469231182508

Fangcong Dong[1], Andrew J Annalora[2], Iain A Murray[1], Yuan Tian[1], Craig B Marcus[2], Andrew D Patterson[1] and Gary H Perdew[1]

[1]Department of Veterinary and Biomedical Sciences, Center for Molecular Toxicology and Carcinogenesis, The Pennsylvania State University, University Park, USA. [2]Department of Environmental and Molecular Toxicology, Oregon State University, Corvallis, USA.

ABSTRACT: The aryl hydrocarbon receptor (AHR) exerts major roles in xenobiotic metabolism, and in immune and barrier tissue homeostasis. How AHR activity is regulated by the availability of endogenous ligands is poorly understood. Potent AHR ligands have been shown to exhibit a negative feedback loop through induction of CYP1A1, leading to metabolism of the ligand. Our recent study identified and quantified 6 tryptophan metabolites (eg, indole-3-propionic acid, and indole-3-acetic acid) in mouse and human serum, generated by the host and gut microbiome, that are present in sufficient concentrations to individually activate the AHR. Here, these metabolites are not significantly metabolized by CYP1A1/1B1 in an in vitro metabolism assay. In contrast, CYP1A1/1B metabolizes the potent endogenous AHR ligand 6-formylindolo[3,2b]carbazole. Furthermore, molecular modeling of these 6 AHR activating tryptophan metabolites within the active site of CYP1A1/1B1 reveal metabolically unfavorable docking profiles with regard to orientation with the catalytic heme center. In contrast, docking studies confirmed that 6-formylindolo[3,2b]carbazole would be a potent substrate. The lack of CYP1A1 expression in mice fails to influence serum levels of the tryptophan metabolites examined. In addition, marked induction of CYP1A1 by PCB126 exposure in mice failed to alter the serum concentrations of these tryptophan metabolites. These results suggest that certain circulating tryptophan metabolites are not susceptible to an AHR negative feedback loop and are likely important factors that mediate constitutive but low level systemic human AHR activity.

KEYWORDS: Ah receptor, AHR, CYP1A1, tryptophan, kynurenine

RECEIVED: April 11, 2023. **ACCEPTED:** May 31, 2023.

TYPE: Original Research Article

FUNDING: The author(s) disclosed receipt of the following financial support for the research, authorship, and/or publication of this article: This work was supported by the National Institutes of Health Grants ES028244 (GHP), ES028288 (ADP), and S10OD021750 (ADP). This work was also supported by the USDA National Institute of Food and Federal Appropriations under Project PEN04772 and Accession number 7000371.

DECLARATION OF CONFLICTING INTERESTS: The author(s) declared no potential conflicts of interest with respect to the research, authorship, and/or publication of this article.

CORRESPONDING AUTHOR: Gary H Perdew, Department of Veterinary and Biomedical Sciences, Center for Molecular Toxicology and Carcinogenesis, The Pennsylvania State University, 309A Life Sciences Building, CMTC, University Park, PA 16802, USA. Email: ghp2@psu.edu

Introduction

The Aryl hydrocarbon receptor (AHR) is a basic helix-loop-helix transcription factor that in vertebrates is activated by ligand binding. In the absence of ligand, the receptor resides in the cytoplasm, complexed with a dimer of heat shock protein 90 and X-associated protein 2.[1,2] Ligand binding induces a conformation change in the AHR within the chaperone complex that mediates nuclear uptake. In the nucleus, the Ah receptor nuclear translocator (ARNT) can displace the chaperone complex leading to the formation of the AHR/ARNT heterodimer.[3] AHR/ARNT is capable of binding to dioxin responsive elements found in the upstream regulatory region of an array of responsive genes. *CYP1A1* was the first gene that was thoroughly characterized as a direct AHR target gene and is almost solely regulated by the AHR.[4] *CYP1B1* is also a direct AHR target gene. More recent studies have demonstrated that the AHR is involved in a myriad of biological activities. For example, the AHR has been shown to exhibit cell- and tissue-specific roles in cell differentiation, such as what has been observed with innate lymphoid cells.[5]

Chemicals that bind to the AHR can be classified as either agonist, partial agonist, antagonist, or selective AHR ligands, with regard to *CYP1A1* induction. Humans are exposed to AHR ligands found in various botanical-foods, exogenous environmental contaminants, produced by microorganisms, or as metabolites synthesized by the host. From a host perspective, tryptophan metabolites appear to be the dominant source of AHR ligands.[6] Tryptophan metabolites generated by the host through the indoleamine 2,3-dioxygenases (IDO1/2) and tryptophan 2.3-dioxygenase (TDO) degradation pathways lead to the production of a number of metabolites, with kynurenine, kynurenic acid, and xanthurenic acid being AHR agonists.[7,8] Tryptophan metabolism by interleukin 4-induced 1 (IL4I1) and glutamic-oxaloacetic transaminase 1 (GOT1) leads to the formation of indole-3-pyruvic acid (I3P), I3P can undergo spontaneous reaction with other compounds, leading to the formation of a variety of compounds, most of which remain to be identified.[9,10] For example, the endogenous ligand 6-formylindolo[3,2b]carbazole (FICZ) has been hypothesized to be generated from I3P and subsequent chemically generated intermediates.[11] Commensal microorganisms in the gastrointestinal tract readily metabolize tryptophan to a variety of metabolites, including tryptamine, indole-3-acetic acid, and indole-3-aldehyde, many of which are also capable of

activating the AHR.[6] Importantly, the production of these metabolites have been shown to play a role in a number of chronic diseases, including blood pressure regulation and cardiovascular disease.[12]

The AHR is considered a promiscuous receptor capable of binding structurally diverse chemicals. However, AHR ligands all have one structural determinant and that is the presence of at least one aromatic ring. High affinity potent AHR agonists have 3 to 5 aromatic rings and are usually planar hydrophobic molecules. For example, polycyclic aromatic hydrocarbons with 4 to 5 aromatic rings (PAH) can activate the AHR, resulting in robust induction of CYP1A1/1B1 expression, which facilitates the formation of hydroxylated PAH metabolites that can then undergo conjugation with glutathione or glucuronide. These PAH conjugates can be excreted to clear an organism of a highly hydrophobic molecule. This paradigm is observed for the endogenous ligand FICZ, which is rapidly eliminated through CYP1A1 metabolism.[13] Considering the importance of the AHR in development, barrier tissue, and immune function, factors that drive AHR constitutive or basal activity are poorly understood. We hypothesized that examination of AHR ligands found at significant serum concentrations may hold a clue and our recent publication has determined that in humans and mice there are 6 major tryptophan metabolites in serum at levels that are capable of significantly activating the AHR either individually, or as a mixture.[14] In this report, we establish that these tryptophan metabolites are not physiological CYP1A1/1B1 substrates and the level of these metabolites in mouse serum are unaffected by PCB-mediated CYP1A1 induction or by a lack of CYP1A1 or any other AHR-dependent metabolic pathway expression in vivo. These results establish that tryptophan metabolites that circulate at significant levels in vivo are not subject to an autoregulatory feedback loop between the AHR and CYP1A1/1B1.

Materials and Methods

Chemicals and reagents

All chemicals unless otherwise stated were from Sigma. Indole-3-propionic acid and indole-3-lactic acid were from Alfa Aesar (Heysham, UK). FICZ was purchased from TOCRIS Biosciences (Bristol, UK). TCDD was kindly provided by Steve Safe (Texas A&M University).

Cell culture

Hepa 1 and Caco2 cells were obtained from American Type Culture Collection and maintained in α-minimal essential medium (Sigma-Aldrich, St. Louis, MO) supplemented with 10% or 15% fetal bovine serum (Hyclone Laboratories, Logan, UT), respectively, and 100 U/mL penicillin and 100 μg/mL streptomycin. Cells were maintained at 37°C in a humidified incubator in 95% air and 5% CO_2.

CYP1A1 microsomal activity assay

Caco2 cells and Hepa 1 cells were treated with 5 nM 2,3,7,8-tetrachlorodibenzo-*p*-dioxin for 24 hours to induce CYP1A1 protein expression. Microsomes were isolated from trypsinized cells washed with phosphate-buffered saline. The cell pellet was resuspended in 0.25 M sucrose, 10 mM Tris-HCl (pH 7.5), with 1 X protease inhibitors (cOmplete Mini, Roche). The cells were homogenized in a Dura-Grind Dounce-Type stainless steel homogenizer (Wheaton). The resulting cell lysate was centrifuged at 10 000×*g* for 10 minutes at 4°C and the supernatant transferred and centrifuged at 100 000×*g* for 90 minutes at 4°C. The microsomal pellet was resuspended in the homogenization buffer, aliquoted and stored at −80°C for CYP1A1 activity assay. Microsomal protein content was determined using the BCA protein assay system (Pierce, Rockford, IL). The P450-Glo CYP1A1/1B1 assay kit, NADPH regeneration system and luciferase assay kit were purchased from Promega (Promega, Madison, WI). P450-Glo assays were performed following manufacturer protocol. Briefly, 25 μL 4X reaction mixtures were assembled, comprising 10 μg microsomal protein, test compounds (4X final concentration), 120 μM luciferin substrate (CEE-luciferin, CYP1A1/B1), and 400 mM potassium phosphate buffer, pH7.4. 4X reaction mixtures were preincubated at 37°C for 10 minutes in white-walled opaque 96-well plates. Reaction mixtures were simultaneously initiated and diluted to 1X by adding of 25 μL NADPH regenerating system. Reactions were incubated at 37°C for 25 minutes. Reactions were terminated by addition of 50 μL luciferin detection reagent. Following incubation at 37°C for 10 minutes, luciferin-based luminescence was quantified using a Synergy HTX multi-mode plate reader (BioTeK, Winooski, VT). Assays were performed in triplicate and data expressed as mean ± SD percent P450 activity relative to vehicle treated.

Mouse experiments

C57BL6/J mice were obtained from Jackson Laboratory (Bar Harbor, ME), bred in-house and maintained on a chow diet. *Ahr*$^{+/-}$, and *Ahr*$^{-/-}$ mice were kindly provided by Dr. Christopher Bradfield (University of Wisconsin-Madison) and bred using female *Ahr*$^{+/-}$ and male *Ahr*$^{-/-}$ mice. Mice were housed on corncob bedding in a temperature- and light-controlled facility and given access to food and water ad libitum. Mice were maintained in a pathogen-free facility and treated humanely with approval from the Animal Care and Use Committee of the Pennsylvania State University and methods were carried out in accordance with approved guidelines. Mice in the 8 to 10-week-old range were utilized in all experiments and were euthanized by over exposure to CO_2, blood was collected after cutting the portal vein. Serum samples were obtained from mice exposed to PCB126 for 6 days as previously described.[15] Briefly, each

mouse was fed a dough pill containing 24 µg/kg PCB126 every 24 hours for 5 days and mice were sacrificed on day 6.

Quantification of tryptophan metabolites in mouse serum

Serum stored at −80°C was thawed on ice, 25 µL was mixed with 100 µL extraction solvent of ice-cold methanol containing isotope labeling standards (indole-3-acetic acid-d4 and kynurenic acid-d5). Mixture was vortexed and stored at −20°C for 30 minutes to precipitate protein. Following centrifugation at 12 000×*g* for 15 minutes at 4°C, the supernatants were collected and subsequently evaporated to dryness (Thermo Scientific, Waltham, MA) and dissolved in 45 µL of 10% acetonitrile. After centrifugation at 12 000×*g* for 15 minutes at 4°C, supernatants were transferred to autosampler vials for LC-MS analysis. Quantitative analysis of tryptophan metabolites was performed by reverse phase UHPLC using a Prominence 20 UFLCXR system (Shimadzu, Columbia, MD) with a water (Milford, MA) BEH C18 column (2.1 × 100 mm × 1.7 µm particle size) maintained at 55°C with a 20 minutes aqueous acetonitrile gradient, at a flow rate of 250 µL/minute. Solvent A was LC/MS grade water with 0.1% formic acid and Solvent B was LC/MS grade acetonitrile with 0.1% formic acid. The initial conditions were 97% A and 3% B, increasing to 45% B at 10 minutes, 75% B at 12 minutes then held at 75% B until 17.5 minutes before returning to the initial conditions. The eluate was delivered into a 5600 (QTOF) TripleTOF using a Duospray™ ion source (all Sciex, Framingham, MA). The results were quantified by comparing the integrated peaks against a standard curve. The recovery and matrix effects for the tryptophan metabolites in mouse serum were used to normalize the quantitative data as previously described.[14]

Computational CYP modeling and docking analysis

The ligand binding affinity and target oxidation sites for a panel of tryptophan metabolites, including FICZ, kynurenine, kynurenic acid, indole-3-acetate, indole-3-lactate, indole-3-propionate, and indole-3-carboxylate were investigated using Autodock Tools 4 and Autodock Vina, and 4 pre-validated, structure-based, computational models of mouse and human CYPs 1A1 and 1B1.[16-18] Crystal structures of human CYP1A1 (4I8V) and human CYP1B1 (3PM0) were utilized to prepare docking models for the human enzymes, and as templates for the mouse homology models, using the SWISS-MODEL server.[19-21] Homology models were validated for overall quality, clashes, and outliers using the SWISS-MODEL server, SAVESv6.0 server (https://saves.mbi.ucla.edu/), and ChimeraX using the ISOLDE plugin.[22-26] Computational docking models for each substrate tested were obtained from the PubChem database and optimized for docking using Autodock Tools. Autodock Vina was run using standard settings (exhaustiveness = 10), using Grid box parameters generated in Autogrid for a 30 to 60 Å^3 docking grid centered on the heme center, as described previously.[27,28] Docking results were analyzed using Autodock Tools 4 and The PyMOL Molecular Graphics System, Version 2.52 Schrödinger, LLC.[29] Active site cavity size was calculated using Caver 3.0.[30] Model quality was validated using an Autodock Vina re-docking analysis with α-naphthoflavone (ANF) in structure-based models. RMSD error was calculated using the program LigRMSD, and models with RMSD error <2.0 Å for ANF (as compared to the crystallographic coordinates) were considered sufficiently accurate for comparative docking studies.[31]

Statistical analysis

Values were expressed as mean ± SEM. Data were compared using one-way analysis of variance with Tukey multiple comparison post-test in GraphPad Prism 9.1.1 (GraphPad Software, Inc, La Jolla, CA, USA) to establish statistical significance between different groups. The value of $P < .05$ was considered statistically significant ($^{****}P < .0001$). All experiments were repeated at least twice.

Results

Tryptophan metabolites are not significant CYP1A1/1B1 substrates/inhibitors

We have developed a microsomal assay system that examines CYP1A1/1B1 enzymatic activity. The microsomes utilized are isolated from either mouse hepatoma or human colonic tumor cell lines treated with TCDD and express significant levels of CYP1A1 as previously described.[32] TCDD prompts a significant increase in CYP1A1 expression but importantly does not exhibit CYP1A1 substrate/inhibitor activity. Secondly, a luciferase substrate (luciferin 6′-chloroethylether, CEE) is used that is highly specific for CYP1A1/1B1. This assay was utilized to test whether tryptophan metabolites that can activate the AHR are also CYP1A1/1B1 substrates. Each metabolite was tested at between 0.1 and 3 µM concentrations, which encompasses the concentrations of the 6 significant tryptophan metabolites that are also AHR ligands found in human serum.[14] None of these metabolites examined exhibited a dose-dependent competition with the CYP1A1/1B1 substrate in either mouse or human microsomal CYP1A1/1B1 assay (Figure 1A and B). In these assays ketoconazole was utilized as a positive control. In addition, FICZ is a potent inhibitor/substrate in this assay, consistent with previous reports (Figure 2).[13]

CYP1A1 modeling of tryptophan metabolites

While the results in Figure 1 would indicate that the tryptophan metabolites are not CYP1A1 substrates or inhibitors, it

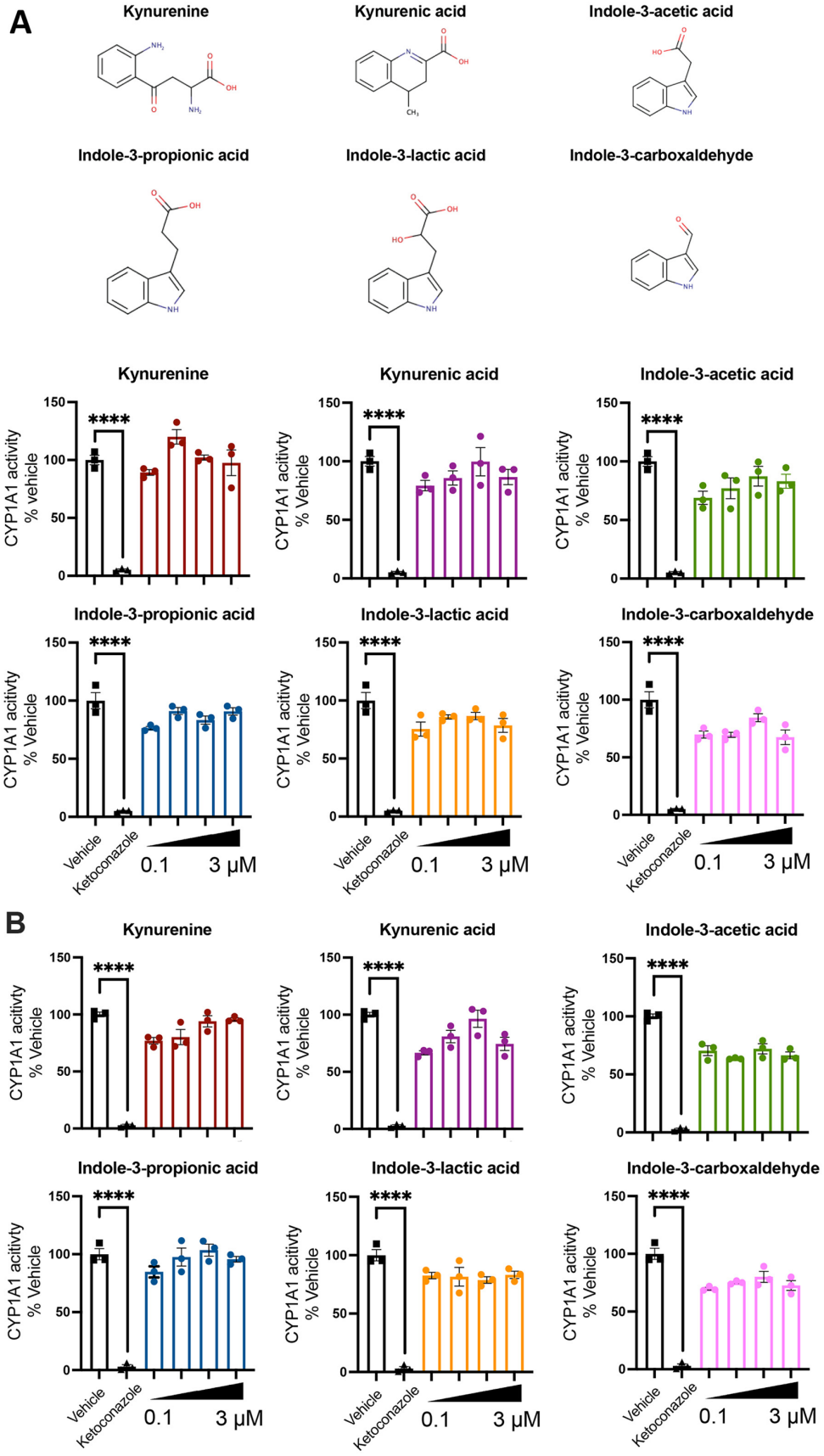

Figure 1. Tryptophan metabolites are not CYP1A1/1B1 competitive substrates/inhibitors. (A) Six tryptophan metabolites; kynurenine, kynurenic acid, indole-3-acetic acid, indole-3-propionic acid, indole-3-lactic acid, or indole-3-carboxaldehyde were co-incubated with Luc-CEE substrate in a Hepa 1 microsomal assay or (B) Caco2 microsomal assay and compared with ketoconazole. The data are mean ± SEM; Tukey's test.
****$P < .0001$.

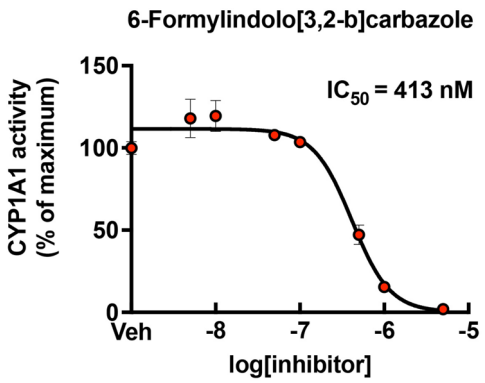

Figure 2. FICZ is a CYP1A1/1B1 inhibitor/competitive substrate. Indicated concentrations of FICZ were co-incubated with Luc-CEE substrate in conjunction with Hepa 1-derived microsomes.

is important to recognize that this is in the context of the conditions utilized in the assay. To gain further insight into whether these metabolites have the potential to be inhibitors/substrates we utilized a molecular modeling docking approach. The substrate binding properties of several tryptophan metabolites, including indole-3-acetate, indole-3-lactate, indole-3-propionate, indole-3-carboxaldehyde, kynurenine, kynurenic acid, and 6-formylindolo[3,2-b]carbazole (FICZ) were studied via computational docking analysis with Autodock Vina. Structure-based docking models of human cytochromes P450 1A1 (hCYP1A1) and 1B1 (h1B1), and homology models of mouse cytochromes P450 1A1 (mCYP1A1) and 1B1 (mCYP1B1) were developed and validated to explore CYP enzyme- and species-specific differences in tryptophan metabolite substrate recognition and metabolism (Figure 3; Table 1).

In Figure 3A, the α-naphthoflavone (ANF) docking, an established CYP1A1 substrate, is shown in the heme-centered, substrate binding pocket of human CYP1A1 (hCYP1A1), with key active site residues depicted. ANF docks in the hCYP1A1 model with low picomolar affinity (−13.7 kcal/mol; K_D = 97 pM; see Table S1), with low root-mean-square error (0.44 Å) compared to the authentic structural coordinates (PDB:4I8V; see Table S1). Comparative tryptophan metabolite docking revealed that the endogenous ligand FICZ also binds hCYP1A1 with low picomolar affinity (−13.8 kcal/mol; K_D = 82 pM; Table 1), in a conformation similar to ANF that positions the C4 carbon 4.4 Å from the heme center (Figure 3B). Similar docking results were obtained for mouse CYP1A1 (mCYP1A1) and human (hCYP1A1) and mouse (mCYP1B1) forms of CYP1B1 (Table 1).

While di-indolyl-compounds like FICZ were found to bind tightly to hCYP1A1 similar to ANF, smaller, aromatic ketone derivatives of tryptophan, like kynurenine, did not (Figure 3A-C). Kynurenine docks hCYP1A1 with low micromolar affinity (−7.9 kcal/mol; K_D = 1.58 μM), in an allosteric pocket formed above the active site, positioning no target carbons within 10 Å of the heme center. Lower affinity docking results for kynurenine that positioned the C4 carbon within 5.1 Å of the heme were also observed (−7.7 kcal/mol; 2.20 μM; not shown), but were less common in general, among all 4 models tested. It is notable that the conversion of kynurenine to the larger, heterocyclic derivative kynurenic acid increased substrate binding affinity to hCYP1A1 over 7-fold (−9.1 kcal/mol; K_D = 212 nM), without forcing the substrate much deeper into the heme pocket (Figure 3D). A secondary docking prediction for kynurenic acid, with ~3-fold reduced affinity (−8.5 kcal/mol; K_D = 577 nM) was also observed, which positioned the C3 carbon only 4.5 Å from the heme center. The low affinity docking results for kynurenine and kynurenic acid suggest they may feasibly be substrates for CYP1A1 and CYP1B1, similar to FICZ, but only when present at higher (micromolar) levels in the cell. This hypothesis is reinforced by convergent docking results for FICZ, kynurenine, and kynurenic acid in all 4 docking models (Table 1).

To further expand our understanding of tryptophan metabolite recognition by the CYP1 family, we next explored the substrate binding properties of 4 additional, microbiome-derived indole compounds, also known to modulate the AHR activity. Tryptophan metabolites, like indole-3-carboxylate, bind hCYP1A1 with, at most, low micromolar affinity (−7.8 kcal/mol, K_D = 1.86 μM) in the same conserved, allosteric site as kynurenine and kynurenic acid (Figure 3E). Indole-3-acetate binds hCYP1A1 with similar, low micromolar affinity (−7.9 kcal/mol, K_D = 1.58 μM), in the same allosteric site, positioning no target carbons within 11 Å of the catalytic center (Figure 3F). Indole-3-lactate, which has a longer side chain than either the carboxylate or acetate derivatives, displayed higher affinity to hCYP1A1 (−8.2 kcal/mol; K_D = 954 nM), despite sharing a similar indole ring binding configuration in the outer, allosteric pocket (Figure 3G). Enhanced, nanomolar range affinity was also observed for indole-3-propionate (−8.4 kcal/mol; K_D = 683 nM), despite sharing a similar docking configuration in the distal, allosteric pocket of the CYP1 family active site (Figure 3H).

Collectively, our docking results suggest that tryptophan metabolites containing only one indole ring, are poor CYP1 family substrates, because of their tendency to bind allosteric sites outside (near the mouth) of the enzyme's narrow, hydrophobic active site. Furthermore, results with kynurenine and kynurenic acid suggest that bacterial oxidations that generate a thiazole ring structure in the tryptophan derivative can increase substrate affinity significantly, improving accessibility to the catalytic center. Indole-derivatives with larger functional groups (eg, lactate or propionate) also revealed enhanced affinity to the enzyme, despite binding far from the heme center. Both CYP1A1 and CYP1B1 have a stronger binding preference for elongated and planar, polycyclic aromatic hydrocarbons, and heterocyclic compounds with multiple rings, than simple aromatics, like kynurenine, and the small microbiome-derived indoles.

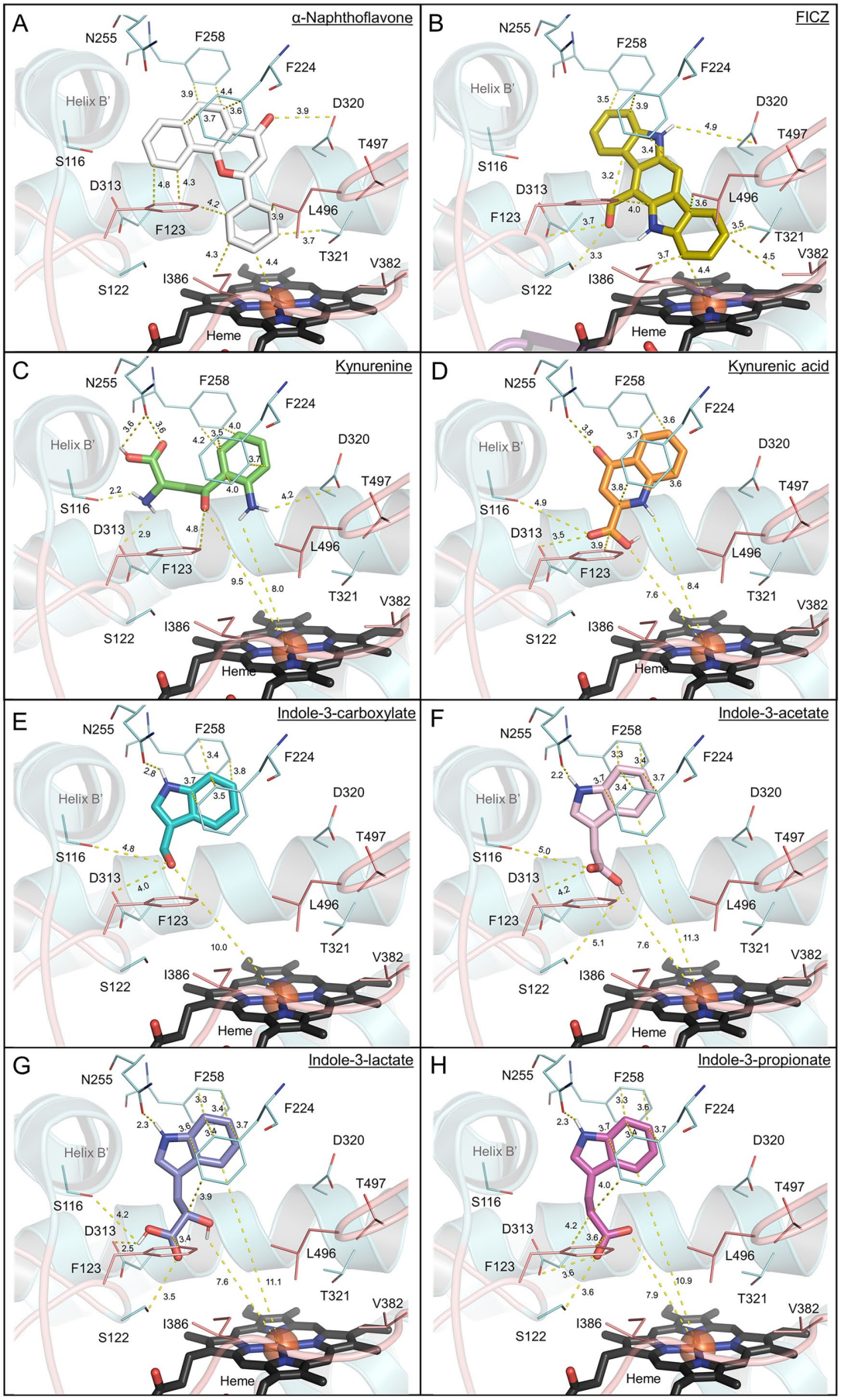

Figure 3. *(Continued)*

Figure 3. Comparative Tryptophan Metabolite Docking Study in Structure-based Model of Human CYP1A1. Substrate binding properties of tryptophan related metabolites, FICZ, kynurenine, kynurenic acid, and 4 gut microbiome-derived indoles (3-carboxylate, 3-acetate, 3-lactate, and 3-propionate) were explored with Autodock Vina and a structure-based human CYP1A1 (hCYP1A1) homology model. (A) Here, α-naphthoflavone (ANF) is shown docked in our computational model of hCYP1A1. The heme-centered active site and substrate binding pocket is highlighted, with key active site residues as shown. Important hydrophobic and electrostatic ligand contact distances to key amino acids are shown (in angstroms; Å; yellow dash). (B) FICZ also binds the hCYP1A1 active site with low picomolar affinity, positioning the C4 carbon 4.4 Å from the heme center, identical to the C4 target carbon distance for ANF. FICZ interacts closely with several highly conserved, active site residues, including F123, F224, F258, D313, T321, V382, I385, and L496. (C) Kynurenine docks in hCYP1A1 in an allosteric pocket above the active site, positioning no target carbons within 10 Å of the heme center. This allosteric site is defined by several well-conserved residues (S116, S122, F123, F224, N255, F258, D313) that converge near the top of the canonical active site, which extends deeper into the enzyme, over the heme center. Lower affinity binding modes for kynurenine that positioned the C4 carbon within 5.1 Å of the heme were also observed. (D) The heterocyclic derivative kynurenic acid did not position the substrate significantly closer to the heme center. A secondary docking prediction for kynurenic acid, with ~3-fold lower affinity was also observed that positioned the C3 carbon 4.5 Å from the heme center. (E) Indole-3-carboxylate binds hCYP1A1 in the same allosteric site as kynurenine. (F) Indole-3-acetate also docks in the same allosteric site, positioning no target carbons within 11 Å of the catalytic center. (G) Indole-3-lactate displayed slightly higher affinity to hCYP1A1 than either the carboxylate or acetate derivatives, but still docked far from the heme. (H) Indole-3-propionate displayed higher affinity for hCYP1A1 than the other indole-derivatives, despite binding in the same allosteric site above the catalytic center.

The lack of AHR expression or AHR activation in mice fails to alter tryptophan metabolite levels

CYP1A1 expression is essentially dependent on AHR expression in mice.[4] Therefore, we tested whether in mice the level of circulating tryptophan metabolites differs in *Ahr*$^{-/-}$, *Ahr*$^{+/-}$, and *Ahr*$^{+/+}$ mice (Figure 4A). We included *Ahr*$^{+/-}$ mice in this analysis because they are from the same litters as *Ahr*$^{-/-}$ mice, this would help rule out genetic differences between different mouse lines. The six tryptophan metabolites analyzed in the in vitro studies were examined in vivo utilizing serum samples from mice on a chow diet. All of the metabolites examined failed to exhibit a significant difference in *Ahr*$^{-/-}$ versus *Ahr*$^{+/-}$ mice. In contrast, comparison of *Ahr*$^{-/-}$ to *Ahr*$^{+/+}$ mice revealed that indole-3-acetic acid was significantly lower in *Ahr*$^{+/+}$ mice, while all other metabolites examined exhibited similar serum levels. The reason is the difference in indole-3-acetate between the *Ahr*$^{-/-}$ to *Ahr*$^{+/+}$ mice is not known. Serum samples from a previous study, where mice were exposed to the potent AHR ligand PCB126 for 5 days, were examined for levels of the 6 tryptophan metabolites.[15] The results indicate that there was no significant difference in the level of these metabolites (Figure 4B), even though *Cyp1a1* was induced ~225-fold in liver.[15]

Discussion

The AHR has evolved as a critical receptor in inducing the metabolism of a wide range of xenobiotics through Phase I and II metabolism. Most high affinity AHR ligands identified for the AHR are exogenous compounds that rapidly induce CYP1A1 expression leading to subsequent metabolic detoxification and inactivation of the AHR ligand. Indeed, CYP1A1 specificity for polycyclic 3 to 5 ring structures evolved to rapidly eliminate potent AHR ligands present in the diet, environment or produced by the host, such as during inflammatory signaling where oxidative stress occurs, thus establishing the concept of an AHR negative feedback loop for potent exogenous agonists.[33] The AHR and CYP1A1 exhibit relatively high constitutive levels in barrier tissues, especially the intestinal tract and lung. Interestingly, in the intestinal tract the highest level of CYP1A1 expression is in the duodenum, which is consistent with the concept that this is where the highest concentration of phytochemicals would exist prior to systemic absorption.[34] Many phytochemicals contain multi-ring structures. For example, flavonoids are widespread across the plant kingdom and as a class generally exhibit either weak AHR agonist or antagonist activity.[35] Flavonoids are also CYP1A1/1B1 substrates and thus are subject to the negative feedback loop.[36] Indeed, the lack of ARNT expression only in the intestinal tract leads to increased AHR activation of CYP1A1 in tissues other than the GI tract, illustrating the importance of intestinal CYP1A1 expression as a barrier to systemic circulation of dietary AHR ligands, which are also subject to the CYP1A1/1B1 negative feedback loop negative.[37]

We have recently identified the major tryptophan metabolites in human and mouse serum that are capable of activating the AHR.[14] Interestingly, of the major tryptophan metabolites that are AHR ligands, only indole-3-propionic acid and 2-oxindole are present due to absorption from the gut. This was a surprising result considering the large number of tryptophan metabolites formed in the GI tract by the microbiome.[38] This implies there are pathways present in tissues forming these metabolites. Considering the importance of the AHR to a variety of developmental, barrier, and immune functions, it would seem reasonable to assume that basal activity would be under control of enzymatic pathways, as would be the case for the circulating tryptophan metabolites examined here. Evidence provided here establishes that tryptophan metabolites are not subject to a negative CYP1A1/1B1 feedback loop. This conclusion is supported by both the in vitro microsomal assays and the lack of change in tryptophan metabolite levels in the absence or presence of CYP1A1 expression in mouse models. Additional support for this concept can also be found in studies on *Cyp1a1, Cyp1a2, Cyp1b1* triple knock-out mice where AHR target genes were not significantly induced, which would be the case if CYP1A1 substrates drove basal AHR

Table 1. Computational docking analysis of tryptophan metabolites in human and mouse CYP1A1 and CYP1B1.

		AUTODOCK VINA			
		STRUCTURE-BASED HOMOLOGY MODELS			
		HUMAN CYP1A1	MOUSE CYP1A1	HUMAN CYP1B1	MOUSE CYP1B1
SUBSTRATE		BINDING ENERGY[a] (KCAL/MOL) [K_D] nM[b]	BINDING ENERGY (KCAL/MOL) [K_D] nM	BINDING ENERGY (KCAL/MOL) [K_D] nM	BINDING ENERGY (KCAL/MOL) [K_D] nM
FICZ	Max[c]	−13.8 [0.082]	−13.5 [0.135]	−14.6 [0.021]	−10.1 [3.98]
	Avg[d]	−13.44 ± 0.37 [0.17 ± 0.10]	−12.98 ± 0.50 [0.43 ± 0.34]	−13.38 ± 1.08 [0.19 ± 0.22]	−9.45 ± 0.83 [197 ± 188]
Kynurenine	Max	−7.9 [1575]	−8.0 [1332]	−8.0 [1332]	−7.5 [3074]
	Avg	−7.49 ± 0.31 [3512 ± 1726]	−7.24 ± 0.45 [4481 ± 2701]	−7.33 ± 0.57 [4874 ± 5940]	−6.88 ± 0.38 [6665 ± 3686]
Kynurenic acid	Max	−9.1 [212]	−9.1 [212]	−9.4 [128]	−8.8 [350]
	Avg	−8.64 ± 0.38 [537 ± 305]	−8.29 ± 0.33 [678 ± 277]	−8.61 ± 0.83 [377 ± 240]	−8.02 ± 0.61 [1879 ± 1567]
Indole-3-carboxylate	Max	−7.8 [1862]	−7.6 [2601]	−8.3 [807]	−7.6 [954]
	Avg	−7.28 ± 0.27 [4353 ± 1835]	−7.34 ± 0.24 [4273 ± 1652]	−7.70 ± 0.27 [2378 ± 889]	−7.22 ± 0.35 [4895 ± 4249]
Indole-3-acetate	Max	−7.9 [1575]	−8.2 [954]	−8.3 [807]	−7.9 [2600]
	Avg	−7.43 ± 0.35 [4049 ± 2259]	−7.47 ± 0.22 [3594 ± 1377]	−7.90 ± 0.36 [1880 ± 1332]	−7.32 ± 0.45 [4006 ± 2874]
Indole-3-lactate	Max	−8.2 [954]	−8.6 [489]	−8.6 [489]	−7.9 [1575]
	Avg	−7.89 ± 0.28 [1769 ± 867]	−7.73 ± 0.59 [3004 ± 2384]	−8.21 ± 0.31 [1053 ± 538]	−7.44 ± 0.38 [3988 ± 2426]
Indole-3-propionate	Max	−8.4 [683]	−8.5 [577]	−9.0 [250]	−8.1 [1127]
	Avg	−7.68 ± 0.48 [2865 ± 1635]	−8.04 ± 0.31 [1378 ± 628]	−8.56 ± 0.30 [587 ± 282]	−6.58 ± 0.93 [27378 ± 28083]

[a]Substrate Binding Energies were derived computationally using Autodock Vina.
[b]Dissociation binding constants (K_D) (in the nanomolar [nM] scale), were derived computationally from Autodock Vina data using the Autodock 4.2 inhibitory constant conversion scale, based on the equation: $y = 0.5982\ln(x) - 12.304$.
[c]Max refers to the low-energy Vina docking solution (in kcal/mol), with the highest predicted binding affinity [K_D], for a given CYP model. If multiple results had the same binding energy, the pose with the closest contact distance to the heme center was selected.
[d]Avg refers to the average or cumulative dissociation constant and binding energy (± the standard deviation) for the Vina docking poses obtained for each individual substrate:model docking combination ($N < 10$).

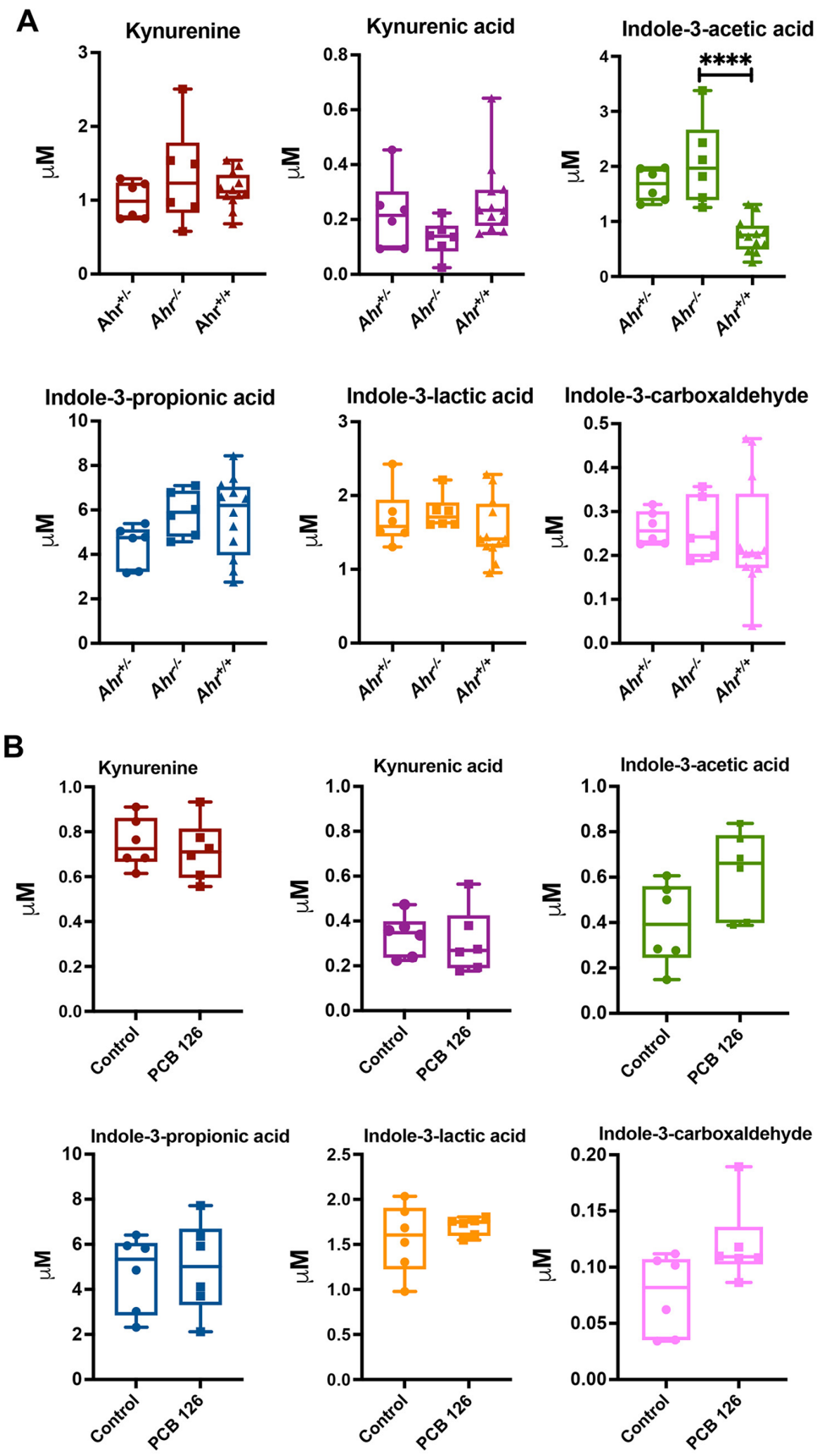

Figure 4. Serum levels of the tryptophan metabolites examined are not altered by AHR phenotype or PCB126-mediated AHR activation in vivo. LC-MS analysis was utilized to quantitate tryptophan metabolites in mouse serum. (A) Concentration of serum tryptophan metabolites were determined in $Ahr^{+/+}$, $Ahr^{+/-}$, and $Ahr^{-/-}$ mice. (B) Concentration of serum tryptophan metabolites in mice treated with PCB126 for 6 days. There were 6 mice in each group in both studies, except the $Ahr^{+/+}$ mice in panel A utilized 11 mice. The data are mean ± SEM; Tukey's test.
****$P < .0001$.

activity.[39] In contrast, if FICZ was the major driver of basal AHR activity, then the lack of CYP1A1/1A2/1B1 would result in a significant increase in AHR target gene expression. Considering that FICZ appears to require a condensation reaction for production that may be dependent on oxidative stress conditions, FICZ-mediated AHR activation may have more of a context-specific targeted function.[11] Another important consideration with tryptophan metabolites is that import and export transporters are likely involved in the cellular levels of these metabolites, which may allow greater control of cell specific AHR activation potential.

We have demonstrated that enzymatically-produced bicyclic tryptophan products (eg, indole, kynurenic acid, 2,8-quinolinediol) are more potent activators of the human AHR as compared to the mouse AHR.[7,40] While the AHR has evolved in humans to be activated by tryptophan metabolites, CYP1A1 appears to have maintained essentially the same substrate specificity for the compounds examined here in both humans and mice. Thus, the ability of human AHR to be activated by various tryptophan metabolites that are not subjected to a negative feedback loop would likely lead to a higher basal CYP1A1 that in turn efficiently metabolize exogenous or endogenous high affinity polycyclic AHR ligands. In addition, tryptophan metabolites would not contribute to excessive redox cycling associated with high level, persistent P450-mediated metabolism. Furthermore, considering the key role that the AHR plays in skin and intestinal differentiation, circulating AHR ligands would continuously facilitate these critical processes. In contrast, within the context of significant basal CYP1A1 activity; potent CYP1A1 substrates like FICZ would be less likely to contribute to the systemic basal AHR activity. This would suggest that endogenously formed compounds such as FICZ would likely exhibit a short half-life in vivo and may not exhibit the characteristics that would result in systemic basal AHR activation. Sustained basal CYP1A1 expression would facilitate immediate detoxification of exogenous metabolites yet not detract from critical constitutive AHR dependent processes mediated by bicyclic tryptophan metabolites.

Acknowledgements

We thank Marcia H. Perdew for critically reviewing of this manuscript.

Author Contributions

F.D., A.A., I.A.M., Y.T., G.H.P. collected and/or analyzed the data. The research was conceived by G.H.P., A.A., C.M., and I.A.M. and supervised by G.H.P., C.M., and A.D.P. The manuscript was written by G.H.P., F.D., I.A.M., and A.A.

Ethics Approval and Consent to Participate

All animal protocols were reviewed and approved by the Animal Care and Use Committee of Penn State University.

Data Availability

The metabolomics data is available at the NIH Common Fund's National Metabolomics Data Repository (NMDR) website, the Metabolomics Workbench, https://www.metabolomicsworkbench.org where it has been assigned Study ID ST002492. The data can be accessed directly via its Project DOI: http://dx.doi.org/10.21228/M8VB03.

Supplemental Material

Supplemental material for this article is available online.

REFERENCES

1. Meyer BK, Pray-Grant MG, Vanden Heuvel JP, Perdew GH. Hepatitis B virus X-associated protein 2 is a subunit of the unliganded aryl hydrocarbon receptor core complex and exhibits transcriptional enhancer activity. *Mol Cell Biol*. 1998; 18:978-988.
2. Chen HS, Perdew GH. Subunit composition of the heteromeric cytosolic aryl hydrocarbon receptor complex. *J Biol Chem*. 1994;269:27554-27558.
3. Beischlag TV, Luis Morales J, Hollingshead BD, Perdew GH. The aryl hydrocarbon receptor complex and the control of gene expression. *Crit Rev Eukaryot Gene Expr*. 2008;18:207-250.
4. Chiaro CR, Patel RD, Marcus CB, Perdew GH. Evidence for an aryl hydrocarbon receptor-mediated cytochrome p450 autoregulatory pathway. *Mol Pharmacol*. 2007;72:1369-1379.
5. Kiss EA, Vonarbourg C, Kopfmann S, et al. Natural aryl hydrocarbon receptor ligands control organogenesis of intestinal lymphoid follicles. *Science*. 2011;334: 1561-1565.
6. Hubbard TD, Murray IA, Perdew GH. Indole and tryptophan metabolism: endogenous and dietary routes to Ah receptor activation. *Drug Metab Dispos*. 2015;43:1522-1535.
7. Dinatale BC, Murray IA, Schroeder JC, et al. Kynurenic acid is a potent endogenous aryl hydrocarbon receptor ligand that synergistically induces interleukin 6 in the presence of inflammatory signaling. *Toxicol Sci*. 2010;115:89-97.
8. Mezrich JD, Fechner JH, Zhang X, Johnson BP, Burlingham WJ, Bradfield CA. An interaction between kynurenine and the aryl hydrocarbon receptor can generate regulatory T cells. *J Immunol*. 2010;185:3190-3198.
9. Bittinger MA, Nguyen LP, Bradfield CA. Aspartate aminotransferase generates proagonists of the aryl hydrocarbon receptor. *Mol Pharmacol*. 2003;64:550-556.
10. Sadik A, Somarribas Patterson LF, Ozturk S, et al. IL4I1 is a metabolic immune checkpoint that activates the AHR and promotes tumor progression. *Cell*. 2020;182:1252-1270.e34.
11. Rannug A. How the AHR became important in intestinal homeostasis-a diurnal FICZ/AHR/CYP1A1 feedback controls both immunity and immunopathology. *Int J Mol Sci*. 2020;21:5681.
12. Paeslack N, Mimmler M, Becker S, et al. Microbiota-derived tryptophan metabolites in vascular inflammation and cardiovascular disease. *Amino Acids*. 2022;54: 1339-1356.
13. Bergander L, Wincent E, Rannug A, Foroozesh M, Alworth W, Rannug U. Metabolic fate of the Ah receptor ligand 6-formylindolo[3,2-b]carbazole. *Chem Biol Interact*. 2004;149:151-164.
14. Morgan EW, Dong F, Annalora A, et al. Contribution of circulating host and microbial tryptophan metabolites towards Ah receptor activation. Preprint. Posted online January 27, 2023. bioRxiv 2023.01.26.525691. doi:10.1101/2023 .01.26.525691
15. Tian Y, Rimal B, Gui W, et al. Early life short-term exposure to polychlorinated biphenyl 126 in mice leads to metabolic dysfunction and microbiota changes in adulthood. *Int J Mol Sci*. 2022;23:8220.
16. Morris GM, Huey R, Lindstrom W, et al. AutoDock4 and AutoDockTools4: automated docking with selective receptor flexibility. *J Comput Chem*. 2009; 30:2785-2791.
17. Trott O, Olson AJ. AutoDock Vina: improving the speed and accuracy of docking with a new scoring function, efficient optimization, and multithreading. *J Comput Chem*. 2010;31:455-461.
18. Eberhardt J, Santos-Martins D, Tillack AF, Forli S. .AutoDock Vina 1.20: new docking methods, expanded force field, and Python bindings. *J Chem Inf Model*. 2021;61:3891-3898.
19. Walsh AA, Szklarz GD, Scott EE. Human cytochrome P450 1A1 structure and utility in understanding drug and xenobiotic metabolism. *J Biol Chem*. 2013;288: 12932-12943.

20. Wang A, Savas U, Stout CD, Johnson EF. Structural characterization of the complex between alpha-naphthoflavone and human cytochrome P450 1B1. *J Biol Chem*. 2011;286:5736-5743.
21. Waterhouse A, Bertoni M, Bienert S, et al. SWISS-MODEL: homology modelling of protein structures and complexes. *Nucleic Acids Res*. 2018;46:W296-W303.
22. Colovos C, Yeates TO. Verification of protein structures: patterns of nonbonded atomic interactions. *Protein Sci*. 1993;2:1511-1519.
23. Bowie JU, Luthy R, Eisenberg D. A method to identify protein sequences that fold into a known three-dimensional structure. *Science*. 1991;253:164-170.
24. Luthy R, Bowie JU, Eisenberg D. Assessment of protein models with three-dimensional profiles. *Nature*. 1992;356:83-85.
25. Pettersen EF, Goddard TD, Huang CC, et al. UCSF ChimeraX: structure visualization for researchers, educators, and developers. *Protein Sci*. 2021;30:70-82.
26. Croll TI. ISOLDE: a physically realistic environment for model building into low-resolution electron-density maps. *Acta Crystallogr D Struct Biol*. 2018;74:519-530.
27. Kim S, Chen J, Cheng T, et al. PubChem in 2021: new data content and improved web interfaces. *Nucleic Acids Res*. 2021;49:D1388-D1395.
28. Annalora AJ, Goodin DB, Hong WX, Zhang Q, Johnson EF, Stout CD. Crystal structure of CYP24A1, a mitochondrial cytochrome P450 involved in vitamin D metabolism. *J Mol Biol*. 2010;396:441-451.
29. *PyMOL*. 2020. Accessed December, 2021. http://www.pymol.org/pymol
30. Chovancova E, Pavelka A, Benes P, et al. CAVER 3.0: a tool for the analysis of transport pathways in dynamic protein structures. *PLoS Comput Biol*. 2012;8:e1002708.
31. Velazquez-Libera JL, Duran-Verdugo F, Valdes-Jimenez A, Nunez-Vivanco G, Caballero J. LigRMSD: a web server for automatic structure matching and RMSD calculations among identical and similar compounds in protein-ligand docking. *Bioinformatics*. 2020;36:2912-2914.
32. Dong F, Murray AI, Annalora A, et al. Complex chemical signals dictate Ah receptor activation through the gut-lung axis. Preprint. Posted online April 5, 2023. bioRxiv 2023.02.22.529529. doi:10.1101/2023.02.22.529529
33. Sridhar J, Goyal N, Liu J, Foroozesh M. Review of ligand specificity factors for CYP1A subfamily enzymes from molecular modeling studies reported to-Date. *Molecules*. 2017;22:1143.
34. Zhou X, Chakraborty D, Murray IA, et al. Aryl hydrocarbon receptor activation coordinates mouse small intestinal epithelial cell programming. *Lab Investig*. 2023;103:100012.
35. Zhang S, Qin C, Safe SH. Flavonoids as aryl hydrocarbon receptor agonists/antagonists: effects of structure and cell context. *Environ Health Perspect*. 2003;111:1877-1882.
36. Hodek P, Trefil P, Stiborova M. Flavonoids-potent and versatile biologically active compounds interacting with cytochromes P450. *Chem Biol Interact*. 2002;139:1-21.
37. Ito S, Chen C, Satoh J, Yim S, Gonzalez FJ. Dietary phytochemicals regulate whole-body CYP1A1 expression through an arylhydrocarbon receptor nuclear translocator-dependent system in gut. *J Clin Invest*. 2007;117:1940-1950.
38. Dong F, Hao F, Murray IA, et al. Intestinal microbiota-derived tryptophan metabolites are predictive of Ah receptor activity. *Gut Microbes*. 2020;12:1-24.
39. Dragin N, Shi Z, Madan R, et al. Phenotype of the Cyp1a1/1a2/1b1-/- triple-knockout mouse. *Mol Pharmacol*. 2008;73:1844-1856.
40. Hubbard TD, Murray IA, Bisson WH, et al. Adaptation of the human aryl hydrocarbon receptor to sense microbiota-derived indoles. *Sci Rep*. 2015;5:12689.